

Synthesis and Reactivity of *ortho*-Carbaborane-Containing Chiral Aminohalophosphines

Sven Stadlbauer,[†] René Frank,[‡] Ilham Maulana,^{†,§} Peter Lönnecke,[†] Barbara Kirchner,[‡] and Evamarie Hey-Hawkins^{*†}

[†]*Institut für Anorganische Chemie, Universität Leipzig, Johannisallee 29, 04103 Leipzig, Germany, and*

[‡]*Wilhelm-Ostwald-Institut für Physikalische und Theoretische Chemie, Universität Leipzig, Linnéstrasse 2, 04103 Leipzig, Germany.* [§]*New address: Department of Chemistry, Faculty of Mathematics and Natural Science Syiah Kuala University, Banda Aceh, 23111, Indonesia*

Received March 5, 2009

The synthesis of chiral *ortho*-carbaboranyl bis(aminoalophosphines) is presented, and spectroscopic and crystallographic data of these compounds are discussed. Furthermore, their reactivity toward alcoholysis was investigated. Quantum chemical calculations showed that the inhibition of methanolysis is of kinetic and not of thermodynamic origin. The disubstitution of the carbaboranes leads to P...P interactions as strong as a hydrogen bond that extremely lower the rate of the methanolysis.

Introduction

Bidentate chiral phosphines have received increasing attention due to their important role as ligands in the development of asymmetric catalytic applications of metal complexes.¹ The steric and electronic properties of the substituents at the two phosphorus atoms play a crucial role,² for example, in determining the relative donor/acceptor ability of the phosphines.³ Dicarba-*closo*-dodecaborane(12) is a particularly interesting potential substituent due to its electron-withdrawing character, electron-delocalizing ability, and bulk.^{4,5}

In the early 1970s, Zakharkin et al. reported the synthesis of monosubstituted *ortho*-carbaboranes with aminochloro- and diamino phosphino substituents.⁶ Hill and Silva-Trivino described the formation of 1,2-bis(*N,N*-dimethylamino-fluorophosphino)-1,2-dicarba-*closo*-dodecaborane(12) as a

decomposition product of a fluorination process.⁷ However, the chemistry of PCI-functionalized dicarba-*closo*-dodecaborane(12) derivatives containing NR₂ groups has hardly been explored. Moreover, sterically hindered tertiary phosphine ligands play a major role in catalysis⁸ by generating unique coordination spheres and promoting reactions that do not occur efficiently with less hindered ligands.⁹ The steric properties of bisphosphines are determined by the substituents at the two phosphorus atoms and the length of the spacer between them.¹⁰ The majority of conventional sterically hindered phosphine ligands, such as P^tBu₃, undergo oxidation in the air. To prevent unwanted conversion to P^v, the phosphines must be handled under special conditions.¹¹

Therefore, the design of sterically encumbered tertiary phosphine ligands that are resistant to oxidation is desirable. Dicarba-*closo*-dodecaboranes are thus attractive backbones from which to construct bulky phosphines. The derivatives of bidentate bisphosphinodicarba-*closo*-dodecaborane(12) form stable chelate complexes.¹² Lately, several

*To whom correspondence should be addressed. E-mail: hey@uni-leipzig.de.
(1) Barbaro, P.; Bianchini, C.; Giambastiani, G.; Parisel, S. L. *Coord. Chem. Rev.* 2004, 248, 2131–2150.
(2) (a) Suresh, C. H.; Koga, N. *Inorg. Chem.* 2002, 41, 1573–1578.
(b) Van Leeuwen, P. W. N. M.; Kamer, P. C. J.; Reek, J. N. H.; Dierkes, P. *Chem. Rev.* 2000, 100, 2741–2769. (c) Marchenko, A. V.; Huffmann, J. C.; Valerga, P.; Tenorio, M. J.; Puerta, M. C.; Caulton, K. G. *Inorg. Chem.* 2001, 40, 6444–6450.
(3) (a) Bowen, R. J.; Garner, A. C.; Berner-Price, S. J.; Jenkins, I. D.; Sue, R. E. *J. Organomet. Chem.* 1998, 554, 181–184. (b) Magee, M. P.; Luo, W.; Hersh, W. H. *Organometallics* 2002, 21, 362–372.
(4) (a) Grimes, R. N. *Carboranes*; Academic Press: New York, 1970.
(b) Bregadze, I. *Chem. Rev.* 1992, 92, 209–223.
(5) Beal, H. In *Boron Hydride Chemistry*; Muetterties, E., Ed.; Academic Press: New York, 1975.
(6) (a) Zakharkin, L. I.; Kazantsev, A. V.; Zhubekova, M. N. *Izv. Akad. Nauk SSSR, Ser. Khim.* 1969, 9, 2056–2057. (b) Zakharkin, L. I.; Zhubekova, M. N.; Kazantsev, A. V. *Zh. Obsh. Khim.* 1971, 41, 588–592. (c) Kazantsev, A. V.; Zhubekova, M. N.; Zakharkin, L. I. *Zh. Obsh. Khim.* 1971, 41, 2027–2033. (d) Zakharkin, L. I.; Zhubekova, M. N.; Kazantsev, A. V. *Zh. Obsh. Khim.* 1972, 42, 1024–1028.

(7) Hill, W. E.; Silva-Trivino, L. M. *Inorg. Chem.* 1978, 17, 2495–2498.
(8) (a) Beare, N. A.; Hartwig, J. F. *J. Org. Chem.* 2002, 67, 541–555.
(b) Aranyos, A.; Old, D. W.; Kiyomori, A.; Wolfe, J. P.; Sadighi, J. P.; Buchwald, S. L. *J. Am. Chem. Soc.* 1999, 121, 4369–4378.
(9) Tsuji, J. *Palladium Reagents and Catalysts, New Perspective for the 21st Century*, 2nd ed.; John Wiley & Sons Ltd.: West Sussex, U. K., 2004.
(10) Tolman, C. A. *Chem. Rev.* 1977, 77, 313–348.
(11) Netherton, M. R.; Fu, G. C. *Org. Lett.* 2001, 3, 4295–4298.
(12) (a) Calhorda, M. J.; Crespo, O.; Gimeno, M. C.; Jones, P. G.; Laguna, A.; Lopez-de-Luzuriaga, J. M.; Perez, J. L.; Veiros, L. F. *Inorg. Chem.* 2000, 39, 4280–4285. (b) Balema, V. P.; Somoza, F. Jr.; Hey-Hawkins, E. *Eur. J. Inorg. Chem.* 1998, 651–656. (c) Crespo, O.; Gimeno, M. C.; Jones, P. G.; Laguna, A.; Villacampa, M. D. *Angew. Chem., Int. Ed.* 1997, 36, 993–995.

metal complexes with five-membered chelate rings were reported to exhibit high catalytic activity.¹³

While nonchiral bisphosphines of dicarba-*closo*-dodecaborane(12) were largely explored,¹⁴ only limited studies on chiral bidentate tertiary phosphine derivatives, in particular, chlorophosphino-substituted compounds,¹⁵ have been reported. Moreover, chiral derivatives with highly electro-negative groups or NR₂ groups at phosphorus were hardly explored.^{7,16}

Here, we describe the synthesis and reactivity of bidentate chiral tertiary aminophosphine ligands containing *ortho*-carbaborane(12) as a backbone. An amino group at the phosphorus atom can result in significant changes in the electronic donor/acceptor properties of the phosphines as well as their steric demand.

Experimental Section

All of the reactions were carried out in an atmosphere of dry nitrogen. The solvents were purified and distilled under nitrogen.¹⁷ The infrared spectra were recorded on a Perkin-Elmer System 2000 FT-IR spectrometer scanning between 400 and 4000 cm⁻¹ using KBr disks. The ¹H, ¹³C, ³¹P, and ¹¹B NMR spectra were recorded on an AVANCE DRX 400 spectrometer (Bruker). The chemical shifts for the ¹H and ¹³C NMR spectra are reported in parts per million at 400.13 and 100.63 MHz with tetramethylsilane as a standard. The chemical shifts for the ³¹P NMR spectra are reported in parts per million at 161.97 MHz (with an 85% H₃PO₄ external standard) and chemical shifts for ¹¹B NMR spectra in parts per million at 128.38 MHz with BF₃·OEt₂ as an external standard. The mass spectra were recorded on an VG Analytics ZAB HSQ spectrometer (FAB) or on a Finnigan MAT MAT8200 spectrometer (EI). The elemental analyses were recorded on a VARIO EL (Heraeus). The melting points were determined in sealed capillaries and are uncorrected.

1,2-Dicarba-*closo*-dodecaborane and 1,7-dicarba-*closo*-dodecaborane are commercially available. PCl₂NMe₂ was purchased from Aldrich and distilled prior to use. PCl₂NEt₂¹⁸ and PCl₂NPh₂¹⁹ were prepared according to the literature.

Computational Details. All electronic structure calculations were carried out with the Turbomole²⁰ program suite. The geometry-optimized structures were obtained by DFT calculations with the BP86 density functional,^{21,22} in which the resolution of identity approximation²³ and the multipole

accelerated resolution of identity²⁴ were used. The TZVPP basis set²⁵ was applied to all atoms. The convergence criterion for the SCF calculations was fulfilled at 10⁻⁸ au, and the length of the gradient vector and geometry optimizations was set to 10⁻⁴ au. The calculations were carried out with and without the conductor-like screening model (COSMO).²⁶ The COSMO parameters were chosen as follows: ε = 30 (for methanol as a solvent) and solvation shell *r*_{solv} = 130 pm. The transition states were counterpoise-corrected.²⁷

X-Ray Crystallographic Analysis. The data were collected on a Siemens CCD diffractometer (SMART,²⁸ data reduction with SAINT²⁹ including the program SADABS³⁰ for empirical absorption correction) or an Oxford Diffraction CCD Xcalibur-S diffractometer (data reduction with CrysAlis Pro³¹ including the program SCALE3 ABSPACK³² for empirical absorption correction) using Mo Kα radiation (λ = 71.073 pm) and ω-scan rotation. The structures were solved by direct methods, and the refinement of all non-hydrogen atoms was performed with SHELXL97.³³ H atoms were located on difference Fourier maps calculated at the final stage of the structure refinement. For disordered solvent molecules in **5a** or the completely disordered molecule **8a/b**, H atoms were calculated on idealized positions. Structure figures were generated with ORTEP³⁴ and DIAMOND-3.³⁵ CCDC 722657, **2a**; 722658, **2b**; 722659, **3b**; 722660, **5a**; 722661, **6a**; 722662, **7b**; and 722663, **8a/b** contain the supplementary crystallographic data for this paper. These data can be obtained free of charge via www.ccdc.cam.ac.uk/conts/retrieving.html (or from the Cambridge Crystallographic Data Centre, 12 Union Road, Cambridge CB2 1EZ, UK; fax: (+44) 1223-336-033; or deposit@ccdc.cam.ac.uk). Crystal data for **2a**, **2b**, **3b**, **5a**, **6a**, **7b**, and **8a/b** can be found in Table 1.

Synthesis of *N,N*-Diisopropylaminodichlorophosphine. Phosphorus trichloride (25 mL, 286 mmol) was dissolved in diethyl ether (600 mL), and the solution was cooled to 0 °C. *N,N*-Diisopropylamine (80 mL, 569 mmol) was added dropwise over 2 h. After complete addition, the reaction mixture was warmed to room temperature and stirred overnight. The ammonium salt was filtered off and then washed with two portions of diethyl ether (2 × 200 mL). Then, the solvent was evaporated and the resulting yellow oil distilled in a vacuum at 2.4 mbar and 54 °C to give 41.3 g (71%) of the product. ¹H NMR (CDCl₃): δ 3.59 (s, br, 2H, CH), 0.87 (d, ³J_{HH} = 6.4 Hz, 12H, CH₃). ³¹P{¹H} NMR (CDCl₃): δ 168.1 (s).

Synthesis of *N,N*-Diisopropylaminodibromophosphine. Phosphorus tribromide (28.2 mL, 300 mmol) was dissolved in diethyl ether (800 mL), and the solution was cooled to 0 °C. *N,N*-Diisopropylamine (84.3 mL, 600 mmol) was added dropwise over 2 h. After complete addition, the reaction mixture was warmed to room temperature and stirred overnight. The ammonium salt was filtered off and then washed with diethyl ether (2 × 200 mL). Then, the solvent was evaporated and the

(13) (a) Cornils, B. In *Applied Homogeneous Catalysis with Organometallic Compounds*; Herrmann, W.A., Ed.; Wiley-VCH: Weinheim, Germany, 2002; Vol. 2. (b) Kumada, M.; Sumitani, K.; Kiso, Y.; Tamao, K. *J. Organomet. Chem.* **1973**, *50*, 319–326.

(14) (a) Paavola, S.; Teixidor, F.; Viñas, C.; Kivekäs, R. *J. Organomet. Chem.* **2002**, *657*, 187–93. (b) Viñas, C.; Benakki, R.; Teixidor, F.; Casabó, J. *Inorg. Chem.* **1995**, *34*, 3844–3845. (c) Teixidor, F.; Viñas, C.; Abad, M. M.; Nuñez, R.; Kivekäs, R.; Sillanpää, R. *J. Organomet. Chem.* **1995**, *503*, 193–203. (d) Contreras, J. G.; Silva-Trivino, L. M.; Solis, M. E. *Inorg. Chim. Acta* **1988**, *142*, 51–54.

(15) (a) Alexander, R. P.; Schroeder, H. J. *Inorg. Chem.* **1963**, *2*, 1107–1110. (b) Balema, V. P.; Blaurock, S.; Hey-Hawkins, E. *Polyhedron* **1999**, *18*, 545–552. (c) Sterzik, A.; Rys, E.; Blaurock, S.; Hey-Hawkins, E. *Polyhedron* **2001**, *20*, 3007–3014. (d) Smith, T. A.; Knowles, H. S. *Inorg. Chem.* **1965**, *4*, 107–111.

(16) Hill, W. E.; Silva-Trivino, L. M. *Inorg. Chem.* **1979**, *18*, 361–364. (17) Perrin, D. D.; Armarego, W. L. F. *Purification of Laboratory Chemicals*, 3rd ed.; Pergamon Press, Oxford, U. K., 1988.

(18) Perich, J. W.; Johns, R. B. *Synthesis* **1988**, *2*, 142–144. (19) Fabis, H.; Babin, M. Z. *Anorg. Allg. Chem.* **1976**, *420*, 65–73.

(20) Ahlrichs, R. *Turbomole*, V5.9; Lehrstuhl für Theoretische Chemie, Universität Karlsruhe: Karlsruhe, Germany, **2006**.

(21) Becke, A. D. *Phys. Rev. A* **1988**, *38*, 3098–3100.

(22) Perdew, J. P. *Phys. Rev. B* **1986**, *33*, 8822–8824.

(23) Eichkorn, K.; Treutler, O.; Öhm, H.; Häser, M.; Ahlrichs, R. *Chem. Phys. Lett.* **1995**, *242*, 652–660.

(24) Sierka, M.; Hogeckamp, A.; Ahlrichs, R. *J. Chem. Phys.* **2003**, *118*, 9136–9148.

(25) EMSL Basis Set Exchange. <https://bse.pnl.gov/bse/portal> (accessed May 2009).

(26) Klamt, A.; Schüürmann, G. *J. Chem. Soc., Perkin Trans.2* **1993**, *5*, 799–805.

(27) Boys, S. F.; Bernardi, F. *Mol. Phys.* **1970**, *19*, 553–556.

(28) SMART; Siemens Industrial Automation, Inc.: Madison, WI, **1993**.

(29) SAINT, version 6.01; Siemens Industrial Automation, Inc.: Madison, WI, **1999**.

(30) Sheldrick, G. M. *SADABS*; University of Göttingen: Göttingen, Germany, **1997**.

(31) *CrysAlis Pro*; Oxford Diffraction Ltd.: Oxfordshire, U. K.

(32) *SCALE3 ABSPACK*; Oxford Diffraction Ltd.: Oxfordshire, U. K.

(33) Sheldrick, G. M. *SHELX97*, release 97-2; University of Göttingen: Göttingen, Germany, 1997; includes SHELXS97 and SHELXL97.

(34) ORTEP3 for Windows; Farrugia, L. J. *J. Appl. Crystallogr.* **1997**, *30*, 565.

(35) Brandenburg, K. *DIAMOND 3*; Crystal Impact GbR: Bonn, Germany.

Table 1. Crystal Data for Compounds 2a, 2b, 3b, 5a, 6a, 7b, and 8a/b

compound	2a	2b	3b	5a	6a	7b	8a/b
empirical formula	C ₁₀ H ₃₀ B ₁₀ ⁻ Cl ₂ N ₂ P ₂	C ₁₀ H ₃₀ B ₁₀ ⁻ Cl ₂ N ₂ P ₂	C ₁₄ H ₃₈ B ₁₀ ⁻ Cl ₂ N ₂ P ₂	C ₂₆ H ₃₀ B ₁₀ ⁻ Cl ₂ N ₂ P ₂ ·C ₇ H ₈	C ₁₂ H ₃₆ B ₁₀ ⁻ N ₂ O ₂ P ₂	C ₁₆ H ₄₄ B ₁₀ ⁻ N ₂ O ₂ P ₂	C ₁₄ H ₃₈ B ₁₀ ⁻ Br ₂ N ₂ P ₂
fw	419.30	419.30	475.40	703.59	410.47	466.57	564.32
T/K	213(2)	210(2)	213(2)	210(2)	210(2)	213(2)	180(2)
cryst syst	monoclinic	triclinic	monoclinic	orthorhombic	monoclinic	orthorhombic	monoclinic
space group	P ₂ ₁ /n	P $\bar{1}$	P ₂ ₁ /c	P ₂ ₁ 2 ₁ 2	C ₂ /c	P ₂ ₁ 2 ₁ 2 ₁	P ₂ ₁
a/pm	715.7(1)	757.2(1)	1782.3(1)	752.7(1)	1433.9(2)	1034.8(2)	773.7(1)
b/pm	1668.0(3)	866.8(1)	983.72(7)	1949.0(4)	1029.0(2)	1495.0(3)	1476.1(3)
c/pm	1915.4(3)	1864.6(3)	1511.4(1)	1228.3(2)	1778.8(3)	1832.4(4)	1202.5(2)
α/deg	90	95.524(3)	90	90	90	90	90
β/deg	92.301(3)	91.078(3)	101.368(1)	90	112.890(4)	90	103.96(1)
γ/deg	90	115.643(2)	90	90	90	90	90
V/nm ³	2.2847(6)	1.0956(3)	2.5979(3)	1.8018(6)	2.4179(7)	2.835(1)	1.3327(4)
Z	4	2	4	2	4	4	2
ρ _{calcd} /Mg m ⁻³	1.219	1.271	1.215	1.297	1.128	1.093	1.406
μ _{Mo-Kα} /mm ⁻¹	0.423	0.441	0.380	0.298	0.190	0.170	3.168
F(000)	872	436	1000	728	872	1000	572
no. of reflns collected	14558	6805	18423	18095	9892	26739	45801
R1/wR2 (I > 2σ(I))	0.0383/0.0879	0.0370/0.0889	0.0339/0.0806	0.0333/0.0790	0.0334/0.0893	0.0375/0.0918	0.0475/0.1086
R1/wR2 (all data)	0.0583/0.0947	0.0455/0.0929	0.0449/0.0863	0.0376/0.0806	0.0415/0.0942	0.0464/0.0971	0.0833/0.1267

resulting yellow oil distilled in a vacuum at 1.0 mbar and 67–68 °C to give 61 g (71%) of the product. Mp: 72–73 °C. ¹H NMR (C₆D₆): δ 3.59 (s, br, 2H, CH), 0.87 (d, ³J_{HH} = 6.40 Hz, 12H, CH₃). ³¹P{¹H} NMR (C₆D₆): δ 170.8 (s).

Synthesis of *rac*-/*meso*-1,2-Bis(*N,N*-dimethylaminochlorophosphino)-1,2-dicarba-*closo*-dodecaborane(12) (1a/1b). *ortho*-Carborane (1.0 g, 57.2 mmol) was dissolved in diethyl ether (30 mL). After cooling to 0 °C, a solution of *n*-BuLi in *n*-hexane (5.90 mL, 13.8 mmol) was added dropwise to the solution. The mixture was warmed to room temperature and stirred for 2 h, during which 1,2-dilithiodicarba-*closo*-dodecaborane(12) was formed as a white solid. The resulting mixture was then added slowly through a cannula to a cooled solution of *N,N*-dimethylaminodichlorophosphine (1.90 mL, 16.5 mmol) in diethyl ether (20 mL). The mixture was stirred overnight at room temperature and then filtered through silica gel. The filtrate was concentrated in a vacuum, and the resulting residue was dissolved in *n*-pentane. Cooling to 4 °C yielded colorless microcrystals of 1a/b. Yield: 1.09 g (43%). Mp: 110–111 °C. ¹H NMR (C₆D₆): δ 3.80–1.80 (m, vbr, 10H, C₂B₁₀H₁₀), 2.24 (d, ³J_{HP} = 6.0 Hz, 12H, CH₃). ¹³C{¹H} NMR (C₆D₆): δ 87.2 (m, ¹J_{CP} + ²J_{CP} = 80.9 Hz, C₂B₁₀H₁₀), 39.6 (m, vbr, CH₃). ³¹P{¹H} NMR (C₆D₆): δ 119.5 (s) and 118.4 (s) (diastereomers). ¹¹B{¹H} NMR (C₆D₆): δ -0.4 (s, 3B, C₂B₁₀H₁₀), -6.5 (s, 3B, C₂B₁₀H₁₀), -9.6 (s, 4B, C₂B₁₀H₁₀). IR (KBr, cm⁻¹): 2963 (m), 2848 (m), 2802 (w) (CH); 2618 (s), 2574 (s) (BH); 1659 (w), 1474 (s), 1447 (w), 1410 (w), 1262 (s), 1171 (m), 1097 (s), 1066 (s), 1023 (s), 981 (s), 901 (w), 864 (w), 801 (s), 733 (w), 688 (m), 621 (w), 560 (w), 472 (m), 445 (w), 410 (m). MS (FAB⁺, 3-nitrobenzyl alcohol matrix) *m/z*: 362.2 (11%, M⁺), 328.2 (100%, M⁺-Cl). Anal. calcd for C₆H₂₂B₁₀Cl₂N₂P₂ (M = 363.19): C, 19.84; H, 6.10; N, 7.71. Found: C, 19.99; H, 6.04; N, 7.59%.

Synthesis of *rac*-/*meso*-1,2-Bis(*N,N*-diethylaminochlorophosphino)-1,2-dicarba-*closo*-dodecaborane(12) (2a/2b). Using the same experimental procedure with *N,N*-diethylaminodichlorophosphine yielded 2 from a concentrated *n*-hexane solution. Yield: 12.7 g (62%). Fractional crystallization gave first 6.8 g (33%) of 2b and then 4.3 g (21%) of 2a.

Data for 2a: Mp: 92 °C. ¹H NMR (CDCl₃): δ 3.52–1.43 (m, vbr, 10H, C₂B₁₀H₁₀), 3.23 and 3.13 (m, 8H, CH₂), 1.08 (t, ³J_{HH} = 4 Hz, 12H, CH₃). ¹³C{¹H} NMR (CDCl₃): δ 87.2 (m, ¹J_{CP} + ²J_{CP} = 106.6 Hz, C₂B₁₀H₁₀), 42.0 (m, vbr, CH₂), 13.4 (s, CH₃). ³¹P{¹H} NMR (CDCl₃): δ 117.2 (s). ¹¹B NMR (CDCl₃): δ -0.5 (d, ¹J_{BH} = 147.0 Hz, 2B, C₂B₁₀H₁₀), -6.8 (d, ¹J_{BH} = 151.0 Hz, 2B, C₂B₁₀H₁₀), -10.0 (d, ¹J_{BH} = 155.1 Hz, 4B, C₂B₁₀H₁₀), -11.2 (m, ¹J_{BH} n.d., 2B, C₂B₁₀H₁₀). IR (KBr, cm⁻¹): 2973 (s),

2936 (s), 2870 (s) (CH); 2621 (s), 2573 (s) (BH); 2006 (w), 1627 (s), 1462 (s), 1441 (m), 1380 (s), 1344 (w), 1291 (m), 1262 (w), 1201 (s), 1165 (s), 1104 (s), 1066 (s), 1023 (s), 971 (w), 947 (s), 918 (w), 831 (m), 795 (s), 744 (m), 730 (m), 668 (m), 621 (m), 564 (m), 502 (s), 489 (s), 448 (m), 417 (m). MS (FAB⁺, 3-nitrobenzyl alcohol matrix) *m/z*: 419 (24%, M⁺), 383 (42%, M⁺-Cl), 347 (100%, M⁺-2Cl), 317 (76%, M⁺-2Cl-C₂H₅). Anal. calcd for C₁₀H₃₀B₁₀Cl₂N₂P₂ (M = 419.30): C, 28.64; H, 7.21; N, 6.68. Found: C, 29.00; H, 7.23; N, 6.46%.

Data for 2b: Mp: 106 °C. ¹H NMR (CDCl₃): δ 3.50–1.35 (m, vbr, 10H, C₂B₁₀H₁₀), 3.19 (m, 8H, CH₂), 1.08 (t, ³J_{HH} = 7 Hz, 12H, CH₃). ¹³C{¹H} NMR (CDCl₃): δ 87.2 (m, ¹J_{CP} + ²J_{CP} = 111.0 Hz, C₂B₁₀H₁₀), 42.1 (m, vbr, CH₂), 13.4 (s, CH₃). ³¹P{¹H} NMR (CDCl₃): δ 117.1 (s). ¹¹B NMR (CDCl₃): δ -0.4 (d, ¹J_{BH} = 147.0 Hz, 2B, C₂B₁₀H₁₀), -6.3 (d, ¹J_{BH} = 138.2 Hz, 1B, C₂B₁₀H₁₀), -7.3 (d, ¹J_{BH} = 140.9 Hz, 1B, C₂B₁₀H₁₀), -9.5 (m, vbr, ¹J_{BH} n.d., 2B, C₂B₁₀H₁₀), -10.4 (d, ¹J_{BH} = 142.0 Hz, 2B, C₂B₁₀H₁₀), -11.9 (m, vbr, 2B, C₂B₁₀H₁₀). IR (KBr, cm⁻¹): 2974 (s), 2936 (s), 2869 (s) (CH); 2619 (s), 2572 (s) (BH); 1461 (s), 1439 (s), 1379 (s), 1342 (m), 1290 (m), 1201 (s), 1164 (s), 1103 (m), 1065 (s), 1022 (s), 971 (m), 947 (s), 830 (m), 793 (m), 728 (m), 667 (m), 619 (m), 561 (w), 500 (s), 448 (m), 423 (w). MS (FAB⁺, 3-nitrobenzyl alcohol matrix) *m/z*: 419 (24%, M⁺), 383 (42%, M⁺-Cl), 347 (100%, M⁺-2Cl), 317 (76%, M⁺-2Cl-C₂H₅). Anal. calcd for C₁₀H₃₀B₁₀Cl₂N₂P₂ (M = 419.30): C, 28.64; H, 7.21; N, 6.68. Found: C, 28.70; H, 7.23; N, 6.61%.

Synthesis of *rac*-/*meso*-1,2-Bis(*N,N*-diisopropylaminochlorophosphino)-1,2-dicarba-*closo*-dodecaborane(12) (3a/3b). Using the same experimental procedure with *N,N*-diisopropylaminodichlorophosphine yielded 3a/b as a mixture of both diastereomers. From a concentrated *n*-hexane solution at room temperature, 3b could be crystallized. Yield: 1.5 g (40%) of 3b. Data for 3b: Mp: 183–184 °C. ¹H NMR (C₆D₆): δ 4.0–2.0 (m, 10H, C₂B₁₀H₁₀), 3.92 (s, br, 2H, N{CH(CH₃)₂}), 2.99 (s, br, 2H, N{CH(CH₃)₂}), 1.08 (s, vbr, 12H, N{CH(CH₃)₂}), 0.92 (s, vbr, 12H, N{CH(CH₃)₂}). ¹³C{¹H} NMR (C₆D₆): δ 89.8 (m, ¹J_{CP} + ²J_{CP} = 110.4 Hz, C₂B₁₀H₁₀), 51.2 (s, N{CH(CH₃)₂}), 46.5 (*pseudo* t, ²J_{CP} = 18.9 Hz, N{CH(CH₃)₂}), 26.2 (s, N{CH(CH₃)₂}), 23.9 (s, N{CH(CH₃)₂}), 21.2 (d, ³J_{CP} = 46.3 Hz, N{CH(CH₃)₂}). ³¹P{¹H} NMR (C₆D₆): δ 113.5 (s). ¹¹B NMR (C₆D₆): δ 0.2 (d, br, ¹J_{BH} = 142.5 Hz, 3B, C₂B₁₀H₁₀), -4.0 (s, ¹J_{BH} n.d., 1B, C₂B₁₀H₁₀), -5.5 (d, br, ¹J_{BH} = 67.3 Hz, 1B, C₂B₁₀H₁₀), -7.1 (s, br, ¹J_{BH} n.d., 1B, C₂B₁₀H₁₀), -9.3 (s, br, ¹J_{BH} n.d., 3B, C₂B₁₀H₁₀), -10.6 (s, br, ¹J_{BH} n.d., 1B, C₂B₁₀H₁₀). IR (KBr, cm⁻¹): 2975 (s), 2937 (m), 2871 (w) (C-H); 2660 (w), 2624 (s), 2605 (s), 2585 (s), 2560 (s) (BH); 1631 (w), 1461 (m),

1392 (s), 1368 (s), 1307 (w), 1245 (m), 1197 (m), 1168 (w), 1149 (w), 1121 (m), 1065 (m), 1021 (m), 963 (m), 878 (w), 852 (w), 831 (w), 798 (w), 734 (w), 663 (w), 640 (w), 620 (w), 531 (m), 501 (w), 462 (s), 433 (w). MS (FAB⁺, 3-nitrobenzyl alcohol matrix) m/z : 475.3 (13, M⁺); 439.3 (30, M⁺ - Cl); 375.2 (35, M⁺ - NⁱPr₂); 340.2 (9, M⁺ - Cl - NⁱPr₂). Anal. calcd for C₁₄H₃₈N₂P₂B₁₀Cl₂ (M = 475.43): C, 35.37; H, 8.06; N, 5.89. Found: C, 35.26; H, 8.19; N, 5.72%.

Synthesis of *rac*-/*meso*-1,2-Bis(*N,N*-diisopropylaminobromophosphino)-1,2-dicarba-*closo*-dodecaborane(12) (4a/4b). Using the same experimental procedure with *N,N*-diisopropylaminodibromophosphine yielded **4** from a concentrated *n*-hexane solution at room temperature. Yield: 0.8 g (40%) of one diastereomer. Data for **4**. Mp: 196–197 °C. ¹H NMR (C₆D₆): δ 4.0–1.8 (m, 10H, C₂B₁₀H₁₀), 3.89 (m, br, 2H, N{CH(CH₃)₂}), 2.93 (m, br, 2H, N{CH(CH₃)₂}), 1.06 (dd, ³J_{HH} = 8.0 Hz, 12H, N{CH(CH₃)₂}), 0.89 (*pseudo* t, 12H, N{CH(CH₃)₂}). ¹³C{¹H} NMR (C₆D₆): δ 88.5 (m, ¹J_{CP} + ²J_{CP} = 116.7 Hz, C₂B₁₀H₁₀), 53.4 (s, N{CH(CH₃)₂}), 46.8 (*pseudo* t, ²J_{CP} = 18.9 Hz, N{CH(CH₃)₂}), 25.9 (s, N{CH(CH₃)₂}), 22.9 (*pseudo* t, ³J_{CP} = 12.1 Hz, N{CH(CH₃)₂}), 21.0 (s, N{CH(CH₃)₂}), 20.0 (s, N{CH(CH₃)₂}). ³¹P{¹H} NMR (C₆D₆): δ 112.8 (s) (one of the two diastereomers). ¹¹B{¹H} NMR (C₆D₆): δ 0.3 (s, br, 3B, C₂B₁₀H₁₀), -4.1 (s, 1B, C₂B₁₀H₁₀), -6.2 (d, br, 1B, C₂B₁₀H₁₀), -8.1 (s, br, 1B, C₂B₁₀H₁₀), -9.3 (s, br, 3B, C₂B₁₀H₁₀), -11.7 (s, br, 1B, C₂B₁₀H₁₀). IR (KBr, cm⁻¹): 2974 (s), 2868 (w) (CH); 2657 (w), 2648 (w), 2627 (w), 2604 (m), 2576 (s), 2563 (m), 2552 (w) (BH); 1459 (m), 1393 (s), 1368 (s), 1308 (w), 1261 (w), 1197 (m), 1167 (m), 1148 (m), 1121 (s), 1062 (m), 1018 (s), 963 (s), 903 (w), 877 (w), 851 (w), 830 (w), 796 (w), 733 (w), 663 (w), 638 (w), 618 (w), 556 (w), 526 (m), 494 (w), 437 (w). MS (EI⁺, 70 eV) m/z : 564.2 (1, M⁺); 484.2 (26, M⁺ - Br); 385.2 (6, M⁺ - Br - NⁱPr₂); 209.9 (11, BrPNⁱPr₂⁺); 100 (21, NⁱPr₂⁺); 43 (100, ⁱPr⁺). Anal. calcd for C₁₄H₃₈B₁₀Br₂N₂P₂ (M = 564.33): C, 29.78; H, 6.79; N, 4.96. Found: C, 30.05; H, 6.88; N, 4.66%.

Synthesis of *rac*-/*meso*-1,2-Bis(*N,N*-diphenylaminochlorophosphino)-1,2-dicarba-*closo*-dodecaborane(12) (5a/5b). Using the same experimental procedure with *N,N*-diphenylaminodichlorophosphine yielded **5b** as the first and the *rac* isomer **5a**·CH₃C₆H₅ as the second crystal fraction.

Data for **5a**. Yield: 11.2 g (32%). Mp: 140 °C. ¹H NMR (CDCl₃): δ 7.33–7.19 (m, 20H, C₆H₅, + C₆H₅ of toluene), 3.52–1.33 (m, vbr, 10H, C₂B₁₀H₁₀), 2.34 (s, CH₃ in toluene). ³¹P{¹H} NMR (CDCl₃): δ 104.3 (s). ¹³C{¹H} NMR (CDCl₃): δ 146.0 (s, *ipso*-C, Ph), 137.8 (s, *ipso*-C, C₇H₈), 129.2 (s, *m*-C, Ph), 129.0 (s, *o*-C, C₇H₈), 128.2 (s, *m*-C, C₇H₈), 127.2 (s, *o*-C, Ph), 126.5 (s, *p*-C, Ph), 125.3 (s, *p*-C, C₇H₈) 86.9 (m, ¹J_{PC} + ²J_{PC} = 104.0 Hz, C₂B₁₀H₁₀), 21.4 (s, CH₃ in C₇H₈). ¹¹B NMR (CDCl₃): δ 0.6 (d, ¹J_{BH} = 128.0 Hz, 2B, C₂B₁₀H₁₀), -5.8 (d, ¹J_{BH} = 144.1 Hz, 4B, C₂B₁₀H₁₀), -10.0 (m, vbr, ¹J_{BH} n.d., 4B, C₂B₁₀H₁₀). IR (KBr, cm⁻¹): 3086 (w), 3065 (m), 3031 (m) (CH); 2630 (s), 2577 (s) (BH); 1945 (w), 1875 (w), 1859 (w), 1798 (w) (Ph); 1594 (s), 1584 (s), 1488 (s), 1450 (m), 1309 (w), 1277 (w), 1235 (s), 1187 (s), 1173 (s), 1157 (m), 1075 (s), 1065 (s), 1029 (s), 1009 (m), 978 (s), 931 (w), 918 (m), 878 (s), 834 (m), 801 (w), 751 (s), 731 (s), 691 (s), 621 (w), 602 (m), 555 (w), 533 (s), 523 (s), 472 (s), 451 (m), 429 (s), 405 (w). MS (FAB⁺, 3-nitrobenzyl alcohol matrix) m/z : 611 (1%, M⁺), 575 (2%, M⁺ - Cl). Anal. calcd for C₂₆H₃₀B₁₀Cl₂N₂P₂·CH₃C₆H₅ (M = 703.63): C, 56.33; H, 5.44; N, 3.98. Found: C, 56.70; H, 5.19; N, 4.01%.

Data for **5b**. Yield: 11.9 g (34%). Mp: 191 °C. ¹H NMR (CDCl₃): δ 7.32–7.20 (m, 20H, Ph), 3.51–1.30 (m, vbr, 10H, C₂B₁₀H₁₀). ³¹P NMR (CDCl₃): δ 103.0 (s). ¹³C{¹H} NMR (CDCl₃): δ 146.2 (s, *ipso*-C, Ph), 129.3 (s, *m*-C, Ph), 127.2 (s, *o*-C, Ph), 126.4 (s, *p*-C, Ph), 87.1 (m, ¹J_{CP} + ²J_{CP} = 104.0 Hz, C₂B₁₀H₁₀). ¹¹B NMR (CDCl₃): δ 0.4 (d, ¹J_{BH} = 130.0 Hz, 2B, C₂B₁₀H₁₀), -5.6 (m, vbr, ¹J_{BH} n.d., 2B, C₂B₁₀H₁₀), -6.2 (m, vbr, ¹J_{BH} n.d., 2B, C₂B₁₀H₁₀), -10.3 (m, vbr, ¹J_{BH} n.d., 4B, C₂B₁₀H₁₀). IR (KBr, cm⁻¹): 3064 (m), 3036 (m) (CH);

2628 (s), 2580 (s), 2552 (s) (BH); 1948 (w), 1868 (w), 1796 (w), 1736 (w), 1662 (w) (Ph); 1591 (s), 1487 (s), 1450 (m), 1393 (w), 1328 (w), 1310 (w), 1279 (w), 1232 (s), 1190 (w), 1108 (w), 1067 (s), 1030 (s), 1011 (m), 978 (s), 914 (w), 905 (w), 878 (m), 837 (m), 800 (w), 756 (s), 694 (s), 623 (w), 603 (w), 536 (s), 577 (s), 448 (m), 427 (m). MS (FAB⁺, 3-nitrobenzyl alcohol matrix) m/z : 611 (7%, M⁺), 575 (8%, M⁺ - Cl). Anal. calcd for C₂₆H₃₀B₁₀Cl₂N₂P₂ (M = 611.49): C, 51.07; H, 4.94; N, 4.47%. Found: C, 51.46; H, 5.10; N, 4.47%.

Synthesis of *rac*-/*meso*-1,7-Bis(*N,N*-diisopropylaminobromophosphino)-1,7-dicarba-*closo*-dodecaborane(12) (8a/b). *meta*-Carbaborane (0.53 g, 3.67 mmol) was dissolved in diethyl ether (15 mL). After cooling to 0 °C, a solution of *n*-BuLi in *n*-hexane (3.0 mL, 7.1 mmol) was added dropwise to the solution. The mixture was warmed to room temperature and stirred for 2 h, during which 1,7-dilithiodicarba-*closo*-dodecaborane(12) formed as a white solid. The resulting mixture was then added slowly through a cannula to a cooled solution of *N,N*-diisopropylaminodibromophosphine (2.21 g, 7.59 mmol) in diethyl ether (15 mL). The mixture was stirred overnight at room temperature. LiBr was filtered off. The solvent was evaporated in a vacuum to dryness, and the resulting residue was extracted with *n*-hexane. The *n*-hexane fraction was concentrated to give crystals of the diastereomeric mixture of **8**. Yield: 0.93 g (45%). Mp: 122–124 °C. ¹H NMR (C₆D₆): δ 4.0–1.8 (m, 10H, C₂B₁₀H₁₀), 3.81 (m, br, 2H, N{CH(CH₃)₂}), 2.87 (m, br, 2H, N{CH(CH₃)₂}), 1.06 (d, ³J_{HP} = 6.4 Hz, 12H, N{CH(CH₃)₂}), 0.93 (s, 12H, N{CH(CH₃)₂}). ³¹P{¹H} NMR (C₆D₆): δ 127.2 (s). ¹³C{¹H} NMR (C₆D₆): δ 78.5 (d, ¹J_{CP} = 105.2 Hz, C₂B₁₀H₁₀), 52.4 (s, N{CH(CH₃)₂}), 46.3 (d, ²J_{CP} = 34.4 Hz, N{CH(CH₃)₂}), 26.0 (s, N{CH(CH₃)₂}), 22.5 (d, ³J_{CP} = 25.6 Hz, N{CH(CH₃)₂}), 21.2 (s, N{CH(CH₃)₂}), 19.9 (s, N{CH(CH₃)₂}). ¹¹B NMR (C₆D₆): δ -2.8 (d, br, ¹J_{BH} = 139.3 Hz, 2B, C₂B₁₀H₁₀), -8.4 (d, ¹J_{BH} = 139.9 Hz, 3B, C₂B₁₀H₁₀), -9.5 (d, br, ¹J_{BH} = 131.8 Hz, 3B, C₂B₁₀H₁₀), -12.3 (d, br, ¹J_{BH} = 168.2 Hz, 2B, C₂B₁₀H₁₀). IR (KBr, cm⁻¹): 2971 (s), 2931 (w), 2870 (w) (CH); 2654 (w), 2592 (s) (BH); 1636 (w), 1459 (m), 1393 (s), 1367 (s), 1309 (w), 1262 (w), 1198 (s), 1166 (m), 1150 (m), 1121 (s), 1078 (m), 1023 (m), 963 (s), 877 (w), 852 (w), 830 (w), 734 (w), 692 (w), 641 (w), 580 (w), 529 (m), 480 (w), 419 (w). MS (EI⁺, 70 eV) m/z : 564.3 (3, M⁺); 484.3 (35, M⁺ - Br); 210 (23, BrPNⁱPr₂⁺); 42.9 (100, ⁱPr⁺). Anal. calcd for C₁₄H₃₈B₁₀Br₂N₂P₂ (M = 564.33): C, 29.78; H, 6.79; N, 4.96. Found: C, 30.09; H, 6.97; N, 4.97%.

Methanolysis of 2b. Compound **2b** (1.0 g, 57.15 mmol) was heated to reflux in triethylamine (1 mL) and methanol (150 mL) for 4 h. The solvent was evaporated and the resulting residue extracted with two portions of *n*-hexane (30 mL). The solution was concentrated and cooled to -8 °C to give colorless crystals of *rac*-1,2-bis(*N,N*-diethylamidomethylphosphonito)-1,2-dicarba-*closo*-dodecaborane(12) (**6a**).

Data for **6a**. Yield: 0.38 g (39%). Mp: 87–88 °C. ¹H NMR (CDCl₃): δ 3.55 (*pseudo* t, ³J_{HP} = 8.0 Hz, 6H, OCH₃), 3.21 and 3.08 (m, 8H, NCH₂CH₃), 3.00–1.50 (m, vbr, 10H, C₂B₁₀H₁₀), 1.09 (t, ³J_{HH} = 8.0 Hz, 12H, NCH₂CH₃). ³¹P{¹H} NMR (CDCl₃): δ 132.4 (s). ¹³C{¹H} NMR (CDCl₃): δ 85.5 (m, ¹J_{CP} + ²J_{CP} = 85.0 Hz, C₂B₁₀H₁₀), 55.2 (*pseudo* t, ²J_{CP} = 12.9 Hz, OCH₃), 40.5 (s, vbr, NCH₂CH₃), 14.5 (s, NCH₂CH₃). ¹¹B NMR (CDCl₃): δ -1.2 (d, ¹J_{BH} = 142.9 Hz, 2B, C₂B₁₀H₁₀), -7.8 (d, ¹J_{BH} = 148.1 Hz, 2B, C₂B₁₀H₁₀), -10.7 (d, ¹J_{BH} = 141.2 Hz, 4B, C₂B₁₀H₁₀), -11.9 (m, vbr, ¹J_{BH} n.d., 2B, C₂B₁₀H₁₀). IR (KBr, cm⁻¹): 2981 (s), 2930 (s), 2882 (s), 2829 (s) (CH); 2617 (s), 2593 (s), 2558 (s) (BH); 2033 (w), 1871 (w), 1773 (w), 1687 (w), 1608 (w), 1508 (w), 1461 (s), 1440 (s), 1380 (s), 1345 (m), 1296 (m), 1205 (s), 1181 (s), 1105 (s), 1063 (s), 1023 (s), 972 (m), 938 (s), 832 (m), 796 (s), 756 (s), 664 (s), 624 (w), 564 (w), 528 (w), 487 (s), 440 (w), 409 (m). MS (FAB⁺, 3-nitrobenzyl alcohol matrix) m/z : 410 (3%, M⁺), 379 (4%, M⁺ - OCH₃). Anal. calcd for C₁₂H₃₆B₁₀N₂O₂P₂

(M = 410.47): C, 35.11; H, 8.84; N, 6.82. Found: C, 35.10; H, 8.69; N, 6.81%.

Methanolysis of 8a/b. Compounds **8a/b** (0.45 g, 0.8 mmol) was heated to reflux in triethylamine (1 mL) and methanol (10 mL) for 4 h. The solvent was evaporated and the residue kept under full vacuum conditions at 70 °C for 2 h to obtain 0.35 g (94%) of **9a/b** as a pale yellow oil. Data for **9a/b**. ^1H NMR (CDCl_3): δ 4.0–1.8 (m, 10H, $\text{B}_{10}\text{H}_{10}$), 3.26 (m, 4H, $\text{N}\{\text{CH}(\text{CH}_3)_2\} + 6\text{H, OCH}_3$), 1.08 (m, 24H, $\text{N}\{\text{CH}(\text{CH}_3)_2\}$). $^{13}\text{C}\{^1\text{H}\}$ NMR (CDCl_3): δ 80.6 (d, $^1J_{\text{CP}} = 73.2$ Hz, $\text{C}_2\text{B}_{10}\text{H}_{10}$), 55.4 (d, $^2J_{\text{CP}} = 28.8$ Hz, OCH_3), 45.0 (m, $\text{N}\{\text{CH}(\text{CH}_3)_2\}$), 24.5 (m, $\text{N}\{\text{CH}(\text{CH}_3)_2\}$). $^{31}\text{P}\{^1\text{H}\}$ NMR (CDCl_3): δ 135.6 (s, br, *rac* + *meso* isomer). ^{11}B NMR (CDCl_3): δ -3.8 (s, br, $^1J_{\text{BH}}$ n.d., 2B, $\text{C}_2\text{B}_{10}\text{H}_{10}$), -8.4 (s, br, $^1J_{\text{BH}}$ n.d., 2B, $\text{C}_2\text{B}_{10}\text{H}_{10}$), -9.6 (s, br, $^1J_{\text{BH}}$ n.d., 4B, $\text{C}_2\text{B}_{10}\text{H}_{10}$), -13.0 (s, br, $^1J_{\text{BH}}$ n.d., 2B, $\text{C}_2\text{B}_{10}\text{H}_{10}$). IR (KBr, cm^{-1}): 2970 (s), 2933 (s), 2829 (m) (CH); 2600 (s) (BH); 2347 (w), 2172 (w), 2055 (w), 1846 (w), 1766 (w), 1656 (w), 1606 (w), 1460 (m), 1393 (m), 1365 (m), 1310 (w), 1260 (w), 1197 (m), 1175 (m), 1155 (w), 1124 (w), 1085 (w), 1038 (m), 970 (m), 913 (w), 875 (w), 850 (w), 824 (w), 795 (w), 735 (m), 695 (w), 640 (w), 589 (w), 521 (m), 440 (w). MS (EI^+ , 70 eV) m/z : 466.4 (100, M^+); 423.3 (65, $\text{M}^+ - ^i\text{Pr}$); 409.3 (18, $\text{M}^+ - ^i\text{Pr} - \text{CH}_2$); 366.3 (30%, $\text{M}^+ - \text{N}^i\text{Pr}_2$); 324.2 (34%, $\text{M}^+ + \text{H} - \text{N}^i\text{Pr}_2 - ^i\text{Pr}$). Anal. calcd for $\text{C}_{16}\text{H}_{44}\text{B}_{10}\text{N}_2\text{O}_2\text{P}_2$ (M = 466.57): C, 41.19; H, 9.50; N, 6.00. Found: C, 40.95; H, 9.74; N, 5.96%.

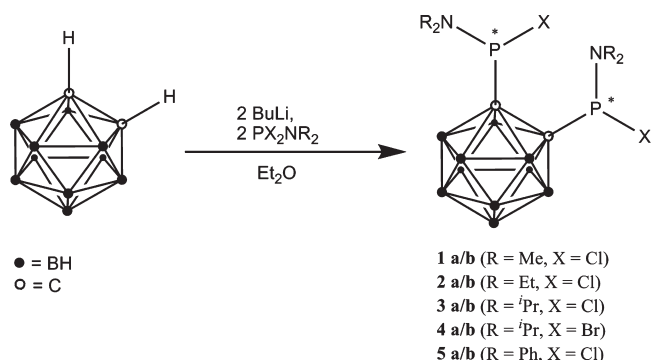
Synthesis of *N,N*-Diisopropylamidomethylchlorophosphite. Methylchlorophosphite (10 mL, 106 mmol) was dissolved in diethyl ether (600 mL), and the solution was cooled to 0 °C. Then, *N,N*-diisopropylamine (29.7 mL, 211 mmol) was added dropwise over 2 h. After complete addition, the reaction mixture was warmed to room temperature and stirred overnight. The ammonium salt was filtered off and then washed with diethyl ether (2 \times 200 mL). Then, the solvent was evaporated and the resulting yellow oil distilled in a vacuum at 10 mbar and 76–78 °C to yield the product as a colorless liquid. Yield: 16.5 g (78%). ^1H NMR (CDCl_3): δ 3.66 (m, 2H, $\text{N}\{\text{CH}(\text{CH}_3)_2\}$), 3.38 (d, $^3J_{\text{HP}} = 14.4$ Hz, 3H, OCH_3), 1.19 (d, $^3J_{\text{HP}} = 6.8$ Hz, 6H, $\text{N}\{\text{CH}(\text{CH}_3)_2\}$), 0.89 (d, $^3J_{\text{HP}} = 6.0$ Hz, 6H, $\text{N}\{\text{CH}(\text{CH}_3)_2\}$). $^{31}\text{P}\{^1\text{H}\}$ NMR (CDCl_3): δ 181.4 (s).

Direct Synthesis of *rac*-/*meso*-1,2-Bis(*N,N*-diisopropylamidomethylphosphonito)-1,2-dicarba-*closo*-dodecaborane(12) (7a/b). *ortho*-Carbaborane (1.0 g, 6.9 mmol) was dissolved in diethyl ether (30 mL). After cooling to 0 °C, a solution of *n*-BuLi in *n*-hexane (5.90 mL, 13.8 mmol) was added dropwise to the solution. The mixture was warmed to room temperature and stirred for 2 h, during which 1,2-dilithiodicarba-*closo*-dodecaborane(12) formed as a white solid. The resulting mixture was then added slowly through a cannula to a cooled solution of *N,N*-dimethylamidomethylchlorophosphite (2.80 mL, 15.6 mmol) in diethyl ether (20 mL). The mixture was stirred overnight at room temperature. LiCl was filtered off, and the solvent was then evaporated to dryness under vacuum conditions. The resulting residue was extracted with *n*-hexane. The combined *n*-hexane fractions were concentrated, and fractional crystallization yielded colorless crystals of the *meso* form **7b**. Yield: 1.4 g (43%), *meso* isomer. Data for **7b**. Mp: 150–151 °C. ^1H NMR (CDCl_3): δ 4.2–1.9 (m, br, 10H, $\text{B}_{10}\text{H}_{10}$), 3.26 (m, 4H, $\text{N}\{\text{CH}(\text{CH}_3)_2\}$, 6H, OCH_3), 1.08 (m, br, 24H, $\text{N}\{\text{CH}(\text{CH}_3)_2\}$). $^{13}\text{C}\{^1\text{H}\}$ NMR (CDCl_3): δ 87.2 (m, $^1J_{\text{CP}} + ^2J_{\text{CP}} = 80.9$ Hz, $\text{C}_2\text{B}_{10}\text{H}_{10}$), 54.6 (m, OCH_3), 45.6 (m, br, $\text{N}\{\text{CH}(\text{CH}_3)_2\}$), 24.3 (m, br, $\text{N}\{\text{CH}(\text{CH}_3)_2\}$). $^{31}\text{P}\{^1\text{H}\}$ NMR (CDCl_3): δ 126.1 (s, *meso* isomer). ^{11}B NMR (CDCl_3): δ -0.3 (s, br, $^1J_{\text{BH}} = 143.3$ Hz, 2B, $\text{C}_2\text{B}_{10}\text{H}_{10}$), -5.3 (s, $^1J_{\text{BH}}$ n.d., 1B, $\text{C}_2\text{B}_{10}\text{H}_{10}$), -7.1 (d, br, $^1J_{\text{BH}} = 150.8$ Hz, 2B, $\text{C}_2\text{B}_{10}\text{H}_{10}$), -10.5 (s, br, $^1J_{\text{BH}}$ n.d., 5B, $\text{C}_2\text{B}_{10}\text{H}_{10}$). IR (KBr, cm^{-1}): 2972 (s), 2930 (m), 2827 (w) (CH); 2625 (s), 2564 (s) (BH); 1456 (m), 1394 (m), 1366 (s), 1198 (s), 1174 (s), 1153 (m), 1121 (s), 1036 (s), 970 (s), 877 (m), 853 (w), 831 (w), 808 (m), 746 (s), 639 (m), 519 (m), 456 (w), 431 (w). MS (FAB^+ , 3-nitrobenzyl

Table 2. $^{31}\text{P}\{^1\text{H}\}$ NMR Data for Compounds 1–5

	1a/b	2a	2b	3a	3b	4a/b	5a	5b
$\delta(^{31}\text{P})$ (ppm)	119.5; 118.4	117.2	117.1	112.4	113.5	114.6; 112.8	104.3	103.0

Scheme 1. Synthesis of Chiral *ortho*-Carbaboranylbis(halophosphines)



alcohol matrix) m/z : 466.4 (2%, M^+); 435.3 (2%, $\text{M}^+ - \text{OCH}_3$); 367.3 (17%, $\text{M}^+ + \text{H} - \text{N}^i\text{Pr}_2$); 304.3 (2%, $\text{M}^+ - \text{PN}^i\text{Pr}_2\text{OCH}_3$); 162.1 (100%, $\text{PN}^i\text{Pr}_2\text{OCH}_3^+$). Anal. calcd for $\text{C}_{16}\text{H}_{44}\text{N}_2\text{O}_2\text{P}_2\text{B}_{10}$ (M = 466.59): C, 41.19; H, 9.50; N, 6.00; Found: C, 41.05; H, 9.86; N, 5.87%.

Results and Discussion

rac-/*meso*-1,2-Bis(*N,N*-dialkylaminohalophosphino)-1,2-dicarba-*closo*-dodecaborane(12)s **1–5** were obtained from dilithiated *ortho*-carbaborane and *N,N*-dialkylaminodichloro- or -dibromophosphines in diethyl ether at 0 °C (Scheme 1). The yields range from about 60 to 70%. In the case of the *N,N*-diethyl-substituted compound, a side product was obtained in 20% yield (according to the $^{31}\text{P}\{^1\text{H}\}$ NMR spectrum, 53.0 ppm), which is probably the 2:2 product. Compounds **1–5** were obtained as mixtures of *rac* and *meso* isomers (ratio 1:1) because of the two chiral phosphorus atoms. Separation of the diastereomers by fractional crystallization from *n*-hexane solutions was possible for **2**, **3**, **4**, and **5**, whereas separation of *N,N*-dimethylamino-substituted compound **1** failed. All compounds were obtained as air- and water-stable colorless solids which are soluble in organic solvents.

Spectroscopic Properties. The $^{31}\text{P}\{^1\text{H}\}$ NMR spectra of **1–5** exhibit two signals due to the two diastereomers, while the proton coupled spectra show only broadening of the signals and, therefore, sometimes only one signal due to overlap (Table 2 gives $^{31}\text{P}\{^1\text{H}\}$ NMR data). Where X-ray crystallography could be employed, the signals could be assigned to the respective diastereomers. The chemical shifts range from about 119 ppm for **1a/b** to 103.0 ppm for **5b**. They show a significant linear trend: with increasing steric demand of the amino group, a marked high-field shift is observed, for example, ca. 119 ppm for dimethylamino-substituted compound **1a/b** and 103.0 ppm for the diphenylamino-substituted compound **5b**. The exchange of chlorine by a bromine atom obviously did not have a significant influence on the chemical shift, as can be seen by comparing **3a/b** with **4a/b**. In general, the signals are shifted by about 45 to

55 ppm to a high field compared to those of the corresponding starting materials, while similar values were observed for the corresponding *rac-meso*-1,2-bis(*tert*-butylchlorophosphino)-1,2-dicarbocloso-dodecaborane (12) (*rac*, 116.7 and *meso*, 116.4 ppm).^{15c}

The diastereomeric mixture of **1** exhibits two doublets for the NMe₂ groups (³J_{PH} 6.0 Hz). Due to the chirality of the phosphino groups, compound **2a** shows two multiplets in the ¹H NMR spectrum for the diastereotopic protons of the CH₂ fragment. This phenomenon is, however, not observed for the CH₂ groups of **2b**, which give rise to only one multiplet. Interestingly, in **3b** the CH₃ groups exhibit not one signal, as expected, but two broad singlets. Probably, the isopropyl groups are inequivalent due to hindered rotation. The four CH groups are also different and exhibit two broad singlets, one at 2.99 and one at 3.92 ppm. Similar observations were made in the ¹³C{¹H} NMR spectrum. Due to the mirror plane in the molecule, four signals for the eight methyl groups are observed. One of the four signals occurs as a pseudotriplet, which became a singlet in the phosphorus-decoupled mode. This observation can be explained by the assumption that two methyl groups have a dihedral angle which allows coupling to phosphorus. Bromo analogue **4** exhibits similar behavior in the NMR spectrum. As no suitable crystals for X-ray crystallography could be obtained of the diastereomers of **4**, we assume that the diastereomer which crystallizes is the *meso* isomer because it exhibits similar NMR spectra to those of the *meso* isomer of **3**.

All compounds show a pseudotriplet for the carbon atoms of the carborane cluster in the ¹³C{¹H} NMR spectrum. For long measuring times, two small satellites can additionally be observed. As reported elsewhere,³⁶ these satellites occur because of the presence of strong P–P coupling. Due to the low natural abundance of ¹³C (1.1%), the majority of molecules which are detected by ¹³C{¹H} NMR only contain one ¹³C atom at this special position. Therefore, these molecules are asymmetric, and the ¹³C nucleus couples with both phosphorus nuclei (¹J_{CP} and ²J_{CP}). This scenario causes a spin system of higher order. By simulating an ABX spin system with SpinWorks,³⁷ the coupling constants J_{PP}, ¹J_{CP}, and ²J_{CP} could be determined for **3b**, and J_{PP} was found to be 280.0 Hz. The reason for the occurrence of strong P–P coupling will be explained below. The distance between the two external signals of the triplets corresponds to the sum of ¹J_{CP} and ²J_{CP}. For **3b**, the sum amounts to 110 Hz. The correct values of the coupling constants can only be determined by simulation with SpinWorks. Subsequently, ¹J_{CP} was found to be 90 Hz and ²J_{CP} 20 Hz.

Molecular Structures of 2a, 2b, 3b, and 5a. While compound **2a** (Figure 1) crystallizes in the centrosymmetric monoclinic space group *P*2₁/*n* with four molecules in the unit cell, compound **2b** (Figure 2) crystallizes in the triclinic space group *P* $\bar{1}$ with two molecules in the unit cell. In the racemic isomer **2a**, the molecule has a noncrystallographic C₂ axis, which bisects the C(1)–C(2) and

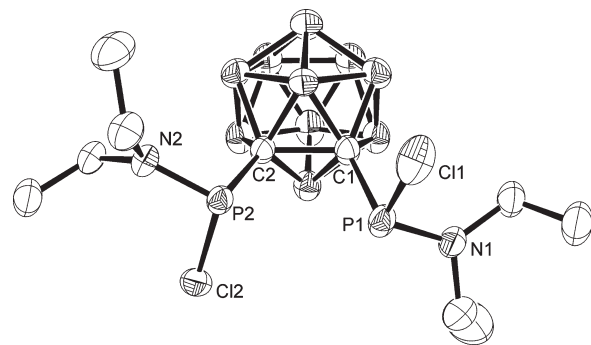


Figure 1. Molecular structure of **2a** (ORTEP with atom labeling scheme; thermal ellipsoids are drawn at the 50% probability level; hydrogen atoms are omitted for clarity; only the *S,S* enantiomer is shown).

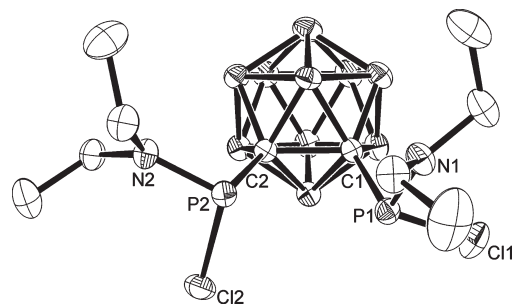


Figure 2. Molecular structure of **2b** (ORTEP with atom labeling scheme; thermal ellipsoids are drawn at the 50% probability level; hydrogen atoms are omitted for clarity).

Table 3. Selected Bond Lengths (pm) and Angles (deg) of **2a**, **2b**, **3b**, and **5a**

	2a	2b	3b	5a
P(1)–C(1)	190.0(2)	191.1(2)	190.3(2)	188.9(1)
P(2)–C(2)	190.8(2)	190.6(2)	189.7(2)	
P(1)–Cl(1)	208.2(8)	207.6(7)	208.87(5)	209.1(6)
P(2)–Cl(2)	207.9(7)	207.5(7)	208.47(6)	
P(1)–N(1)	164.6(2)	164.4(2)	165.4(1)	166.7(1)
P(2)–N(2)	164.3(1)	164.6(1)	164.4(1)	
C(1)–C(2)	170.6(2)	170.4(2)	172.6(2)	174.7(3)
N(1)–P(1)–C(1)	104.7(7)	106.1(7)	105.30(7)	104.9(6)
N(1)–P(1)–Cl(1)	103.9(6)	104.1(6)	103.65(5)	106.0(5)
C(1)–P(1)–Cl(1)	97.5(6)	96.9(5)	98.32(5)	98.3(5)
N(2)–P(2)–C(2)	104.0(7)	104.3(7)	106.81(6)	
N(2)–P(2)–Cl(2)	103.5(5)	103.6(6)	104.61(5)	
C(2)–P(2)–Cl(2)	96.9(5)	97.4(5)	97.80(5)	
C(3)–N(1)–C(5)	116.7(2)	116.9(2)	116.7(1)	116.2(1)
C(3)–N(1)–P(1)	126.9(2)	126.4(1)	126.2(1)	127.7(1)
C(5)–N(1)–P(1)	115.8(1)	115.7(1)	114.5(1)	114.1(1)

B(4)–B(7) bonds; in the *meso* isomer **2b**, the molecule has a noncrystallographic pseudomirror plane on which the atoms B(2), B(3), B(8), and B(9) are located. Due to the presence of an inversion center in the space group, both enantiomeric forms of **2a** (*R,R* and *S,S*) are present in the unit cell. Selected bond lengths and angles are listed in Table 3.

Single crystals of the *meso* isomer of **3** were obtained by recrystallization from *n*-hexane at room temperature. Compound **3b** (Figure 3) crystallizes in the monoclinic space group *P*2₁/*n* with four molecules in the unit cell. The molecule has a noncrystallographic mirror plane, which bisects the C–C bond of the cluster. Compound **5a** crystallizes in the orthorhombic space group *P*2₁2₁2 with two formula units and two molecules of toluene in the unit cell. The molecule of **5a** (Figure 4) has a

(36) Bauer, S.; Tschirschwitz, S.; Lönnecke, P.; Frank, R.; Kirchner, B.; Clarke, M. L.; Hey-Hawkins, E. *Eur. J. Inorg. Chem.*, in press.

(37) Marat, K. *SpinWorks*, version 2.3; University of Manitoba: Winnipeg, Canada, 2004.

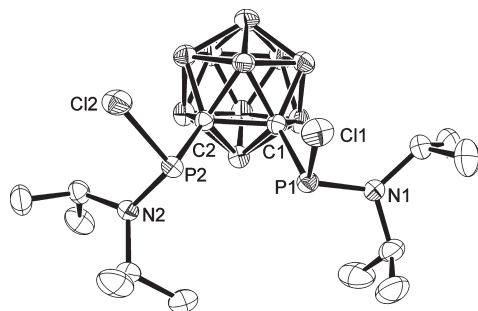


Figure 3. Molecular structure of **3b** (ORTEP with atom labeling scheme; thermal ellipsoids are drawn at the 50% probability level; hydrogen atoms are omitted for clarity; only the *R,R* enantiomer is shown).

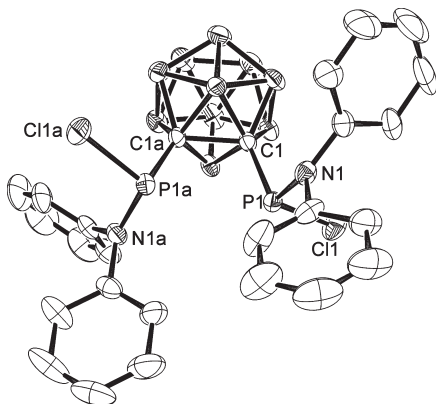


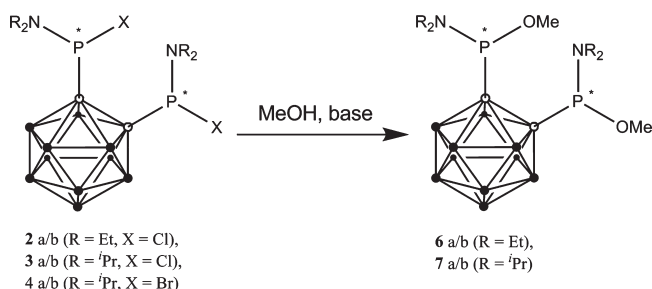
Figure 4. Molecular structure of **5a** (ORTEP with atom labeling scheme; thermal ellipsoids are drawn at the 50% probability level; hydrogen atoms are omitted for clarity; only the *R,R* enantiomer is shown).

crystallographic C_2 axis, which bisects the C(1)–C(1a) and B(4)–B(4a) bonds. Selected bond lengths and angles are collected in Table 3.

In **2a**, **2b**, **3b**, and **5a**, each phosphorus atom has pyramidal coordination by one nitrogen atom, one carbon atom of the carbaborane cluster, one chlorine atom, and the lone pair of electrons. The C–C bond length of the cluster ranges from 170.6 (**2a**) to 174.7 pm (**5a**) and is therefore in the same range as in similar compounds.^{12b,14} In general, the bond lengths and angles of **2a/b**, **3b**, and **5a** show no remarkable deviations from comparable structures. Nevertheless, the P–Cl bond lengths in **2a/b**, **3b**, and **5a** are longer by approximately 4 pm than those observed in *rac*-1,2-(PPhCl)₂(C₂B₁₀H₁₀) (205.1(1) pm)^{15b} and *rac*- and *meso*-1,2-(P^{*t*}BuCl)₂(C₂B₁₀H₁₀) (207.4(9)/207.0(8) and 207.0(9)/205.8(9) pm).^{15c} The comparison shows the influence of the NR₂ groups on the electronic properties of the phosphorus atoms, which are reflected in changes in the P–Cl bond lengths.

Methanolysis of the Halophosphines. The methanolysis of carbaboranylchlorophosphines **2–5** (Scheme 2) was studied for further functionalization of the phosphorus atom. Due to the P–Cl bond, the compounds were expected to undergo rapid reactions with O or N nucleophiles. This was attempted by treating the *meso* isomer **3b** with an excess of 4.7 equiv of methanol and pyridine at room temperature. Unexpectedly, the reaction proceeds very slowly. After 18 h, only about 10% of the desired product and 90% of the starting material were observed in the ³¹P{¹H} NMR spectrum. Therefore, a

Scheme 2. Methanolysis of Carbaboranylbis(aminohalophosphines)



large excess of 120 equiv of methanol was added to the reaction mixture. After a further 24 h, 62% of **3b** was still left and about 20% of the product was observed, besides a significant amount of decomposition products. To accelerate the conversion, 2 equiv of 1*H*-1,2,4-triazole were added to the reaction mixture. After a further 5 days at room temperature, about 10% of **3b** was still unconverted. The reaction mixture contained about 60% product and nearly 30% decomposition products. Instead of solely one signal for the *meso* product, a mixture of *rac* and *meso* isomers in a ratio of 1:6 was detected. The occurrence of the *rac* isomer shows that methanolysis surprisingly proceeds with retention at some phosphorus atoms. The reaction with **3b** was also conducted under reflux conditions in methanol as a solvent and triethylamine or pyridine as a base. In both cases, decomposition was observed to a large extent, and only minor formation of **7** was observed. Surprisingly, the reaction with the more reactive bis(bromophosphine) derivative **4a/b** led under reflux for 3 h to very similar results. The same problems were observed when **2a**, **2b**, and a bis(*tert*-butylchlorophosphine) derivative³⁸ were treated with methanol.

These findings are in contrast to the observation that carbaboranylmonochlorophosphines smoothly underwent alcoholysis with different alcohols by stirring overnight at room temperature to yield the expected products.³⁹ The extended reaction time and the formation of byproducts indicate that methanolysis in the 1,2-disubstituted derivatives is prevented to a certain extent. Theoretical investigations of the bisphosphines were therefore carried out to account for the inhibited methanolysis.

Computational Approach to Inhibited Methanolysis. In general, incomplete conversion of the reactants can be traced back to either thermodynamics or kinetics, both of which are to be considered apart from each other. The thermodynamic discussion focuses on the calculation of the Gibbs energy of the reaction $\Delta_R G^\circ$. A kinetic investigation encompasses a transition-state (TS) search of the most likely reaction path and includes the calculation of the activation barrier $\Delta_R G^\ddagger$. Herein, the computational studies are based on numerous simplifications which are presented in detail in the Supporting Information.

We employed the known reactions of monosubstituted *ortho*-carbaboranes as a benchmark, because they are

(38) Maulana, I. Ph.D. thesis, Universität Leipzig, Leipzig, Germany, 2005.

(39) Tschirschwitz, S.; Lönnecke, P.; Hey-Hawkins, E. *Organometallics* 2007, 26, 4715–4724.

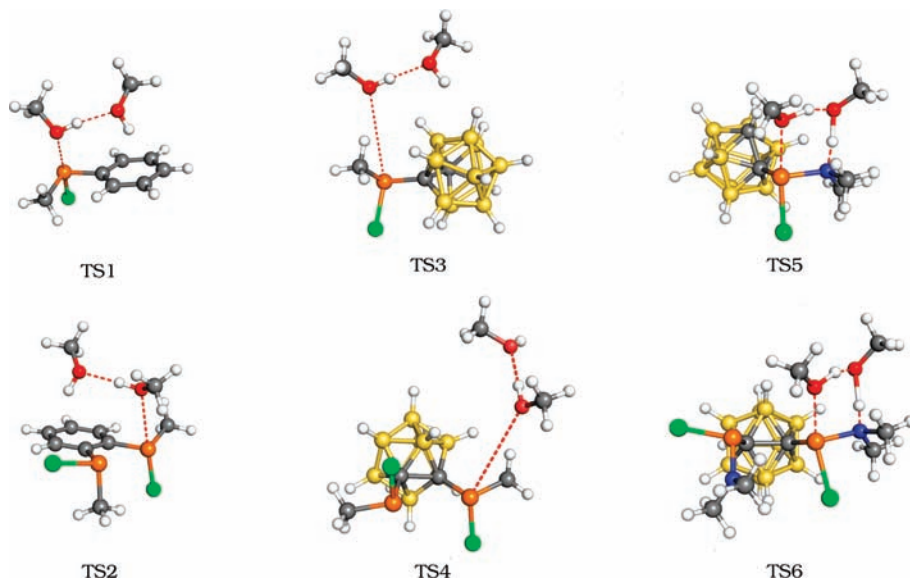


Figure 5. Investigated monosubstituted derivatives of benzene and *ortho*-carbaborane (top) and their disubstituted analogues (bottom). The illustration shows the attack of methanol at phosphorus. Boron (tan), carbon (gray), chlorine (green), hydrogen (white), nitrogen (blue), oxygen (red), phosphorus (orange). Note the distinct geometry for the nitrogen-substituted TS5 and TS6.

Table 4. Differences in the Free Activation Enthalpies for the Transition States and the Resulting Relative Rate Constants, Obtained from Eyring's Equation and Calculated for Standard Conditions

	TS2/TS1	TS4/TS3	TS6/TS5
$\Delta(\Delta G^\ddagger)$ [kJ/mol]	3.8	10.0	13.8
k_{rel}	$k_{\text{rel}} = \frac{k_{\text{TS2}}}{k_{\text{TS1}}} = \frac{1}{4.6}$	$k_{\text{rel}} = \frac{k_{\text{TS4}}}{k_{\text{TS3}}} = \frac{1}{56.5}$	$k_{\text{rel}} = \frac{k_{\text{TS6}}}{k_{\text{TS5}}} = \frac{1}{261.7}$

certainly known to proceed with respect to thermodynamics and kinetics. The thermodynamics and kinetics of the disubstituted derivatives were calculated and compared to the monosubstituted ones.

Thermodynamics. The values of $\Delta_{\text{R}}G^\circ$ for the methanolysis of the mono- and disubstituted *ortho*-carbaborane derivatives were found to be of similar magnitude. Because $\Delta_{\text{R}}G^\circ < 0$, thermodynamic hindrance could be excluded for the disubstituted derivatives, and a kinetic investigation was carried out.

Kinetics. The transition states (Figure 5) were found to be solvent-supported, because methanol is a solvent and a nucleophile at the same time. We only obtained reasonable transition states when a dimer of methanol was simulated to attack, whereas attempts with a single molecule of methanol failed. Table 4 gives differences in the free activation enthalpies for the transition states and the resulting relative rate constants.

The entries suggest that the alcoholysis of the disubstituted derivatives proceed at rates which are lower than those of the monosubstituted compounds. These findings are in accordance with the experiment. The alcoholysis of the disubstituted *ortho*-carbaborane bearing P(Cl)(Me) substituents is 57 times slower than its monosubstituted analogue (TS4 and TS3). This effect is even more pronounced in case of P(Cl)(NMe₂) substituted compounds. Here, the alcoholysis of the disubstituted compound is 262 times slower compared to the monosubstituted derivative (TS6 and TS5). It was clearly demonstrated that the problems in alcoholysis are of kinetic origin and arise from the 1,2-disubstitution pattern. The kinetic inhibition is especially distinct in the case of the carbaborane

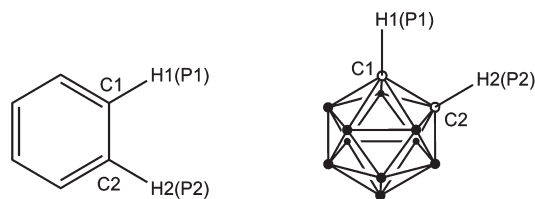


Figure 6. Numbering of the atoms in disubstituted phenyl and carbaborane derivatives.

derivatives and, in turn, even more pronounced in the case of the amino derivatives. We assume that inhibition occurs for two reasons: the steric demand of the carbaborane moiety and interactions between the two phosphorus atoms.

P...P Interactions. For further investigation, we inspected the geometrically optimized structures and compared them to the unsubstituted scaffolds (Figure 7). All disubstituted structures exhibit distances between the phosphorus atoms shorter than the sum of the van der Waals radii ($2 \times 190 \text{ pm}$)⁴⁰ and attraction of the phosphorus moieties to each other, indicated by compression of the covalent angles (Table 5).

The numbering of the atoms is in accordance with Figure 6.

These findings clearly show that attractive interactions between the phosphorus moieties occur. Further indications for the interactions was obtained by means of the shared electron number (SEN) values. The SEN values between the phosphorus atoms (Figure 7) range from 0.026 to 0.059 and are therefore on the same order of magnitude as a hydrogen bond in a simulated water dimer (0.040). Visualization of the canonical molecular orbitals for Ia–III shows significant overlap of orbital fragments with the same sign and therefore rationalizes attraction between the phosphorus moieties (Figure 7).

(40) (a) Pauling, L. *The Nature of the Chemical Bond*, 3rd ed.; Cornell University Press: Ithaca, NY, 1960; p 260. (b) Batsanov, S. S. *Russ. J. Inorg. Chem.* **1991**, *36*, 1694–1708.

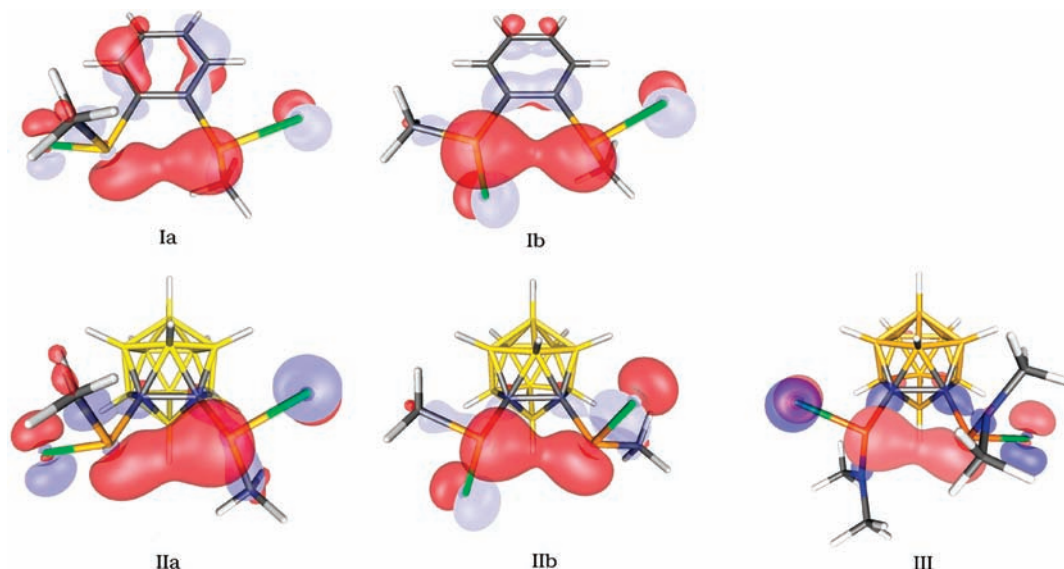


Figure 7. Geometrically optimized disubstituted compounds. P(Cl)(Me) derivatives occur in two conformations, denoted by a and b, respectively. Canonical molecular orbitals visualized with a spatial probability of 95%. The red and blue areas symbolize a positive or negative sign of the wave function, respectively. Ia (HOMO-1), Ib (HOMO-1), IIa (HOMO-2), IIb (HOMO-2), and III (HOMO-3); boron (tan), carbon (gray), chlorine (green), hydrogen (white), and phosphorus (orange).

Table 5. Calculated Distances and Angles

	distance H1–H2 (P1–P2) [pm]	bond angle H–C–C (P–C–C) [deg]
<i>o</i> -C ₆ H ₄	248.9	120.0
<i>o</i> -(–CB ₁₀ H ₁₀ C–)	258.7	116.3
Ia	301.2	115.4
IIa	307.3	111.0
Ib	317.5	118.2
IIb	324.7	113.5
III	308.5	110.6

The quantum chemical considerations are consistent with a couple of experimental observations. The geometry is demonstrated for **3b** as a selected example (Figure 3). The respective distance P1···P2 amounts to 314.6 pm. The P1–C1–C2 angle is 113.65(9)°, and the P2–C2–C1 angle is 109.75(9)°. The extraordinarily high P–P coupling constant described above is in accordance with the orbital and population analysis. In accordance with this theory, a *meta*-carbaborane derivative should react without any problems. Therefore, the *meta*-carbaborane analogue of **4** was synthesized according to the procedure described for the *ortho*-carbaborane. The resulting compound, **8**, was formed as a mixture of *rac* and *meso* isomers.

Molecular Structure of 8a/b. The compound crystallizes in the monoclinic space group *P*2₁ with two molecules in the unit cell. The crystal contains about 80% *rac* isomer and 20% *meso* isomer. The molecular structure (without disorder, only the *R,R* enantiomer is shown) is presented in Figure 8; selected bond lengths and angles are listed in Table 6. The molecule exhibits a noncrystallographic C₂ axis, which bisects the center of the B(2)–B(3) bond and the center of the B(9)–B(10) bond.

The P–C bond length shows no difference in comparison with the corresponding *ortho*-carbaborane derivatives **2a/b**, **3b**, and **5a**. The P–Br bonds are slightly shorter (ca. 227 pm) than the P–Br bonds in dibromotetraphosphatetetracyclonane

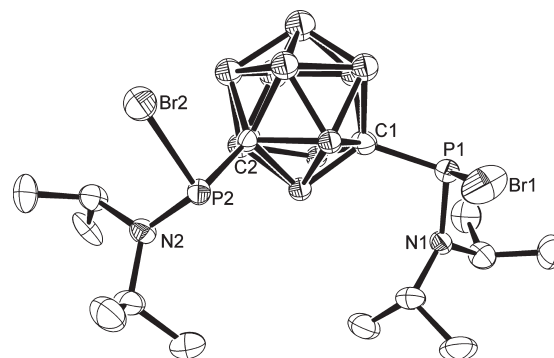


Figure 8. Molecular structure of **8a/b** (ORTEP with atom labeling scheme; thermal ellipsoids are drawn at the 50% probability level; hydrogen atoms are omitted for clarity; only the *R,R* enantiomer is shown).

Table 6. Selected Bond Lengths (pm) and Bond Angles (deg) of **8a/b**

bond lengths [pm]		bond angles [deg]	
Br(1)–P(1)	227.3(1)	N(1)–P(1)–C(1)	106.8(2)
P(1)–N(1)	164.5(3)	N(1)–P(1)–Br(1)	104.2(1)
P(1)–C(1)	188.2(4)	C(1)–P(1)–Br(1)	99.2(1)
Br(2)–P(2)	227.5(2)	N(2)–P(2)–C(2)	107.3(6)
P(2)–N(2)	164.9(9)	N(2)–P(2)–Br(2)	105.7(5)
C(1)–C(2)	188(1)	C(2)–P(2)–Br(2)	98.4(3)
		C(3)–N(1)–C(6)	116.7(3)
		C(3)–N(1)–P(1)	126.2(2)
		C(6)–N(1)–P(1)	115.2(2)

derivatives (228.6(2) and 231.2(2) pm⁴¹ or 228.7(1) and 231.3(1) pm⁴²). On the other hand, they are in good accordance with the P–Br bond lengths found for 1,8-bis-(dibromophosphanyl)naphthalene (between 222.53(9) and 227.37(9) pm).⁴³

(41) Asmus, S. M. F.; Bergsträssler, U.; Regitz, M. *Synthesis* **1999**, 9, 1642–1650.

(42) Dietz, J.; Schmidt, T.; Renner, J.; Bergsträssler, U.; Tabellion, F.; Preuss, F.; Binger, P.; Heydt, H.; Regitz, M. *Eur. J. Org. Chem.* **2002**, 1664–1676.

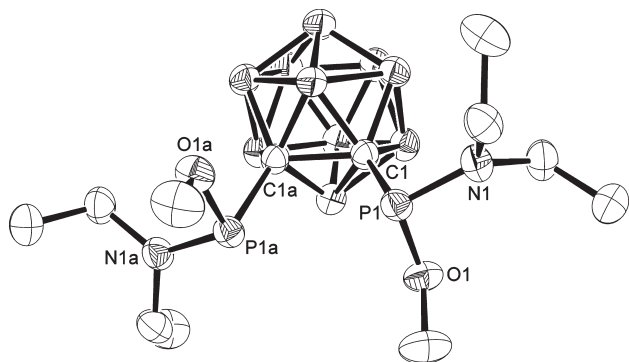


Figure 9. Molecular structure of **6a** (ORTEP with atom labeling scheme; thermal ellipsoids are drawn at the 50% probability level; hydrogen atoms are omitted for clarity; only the *R,R* enantiomer is shown).

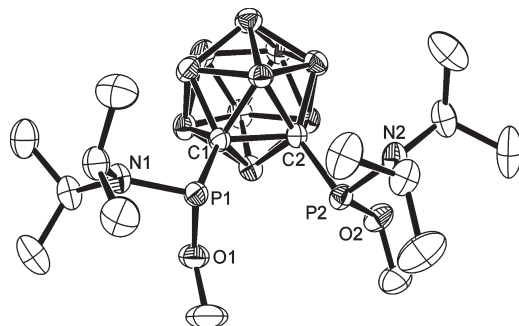
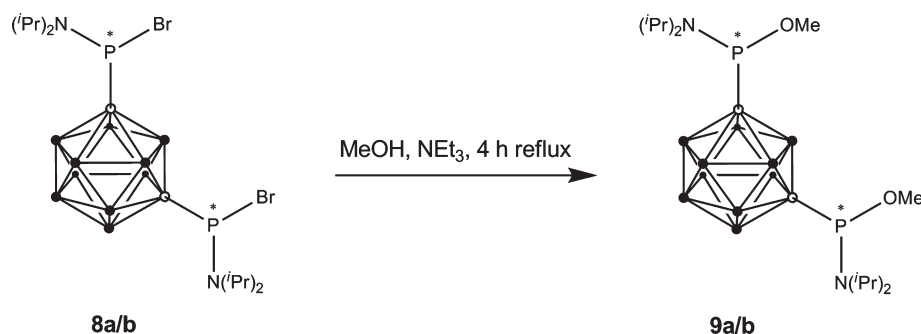


Figure 10. Molecular structure of **7b** (ORTEP with atom labeling scheme; thermal ellipsoids are drawn at the 50% probability level; hydrogen atoms are omitted for clarity).

Table 7. Selected Bond Lengths (pm) and Bond Angles (deg) of **6a** and **7b**

	6a	7b
P(1)–O(1)	162.9(1)	164.0(1)
P(1)–N(1)	165.4(1)	166.5(2)
P(1)–C(1)	190.3(1)	191.1(2)
P(2)–O(2)		164.7(1)
P(2)–N(2)		166.4(2)
P(2)–C(2)		191.3(2)
C(1)–C(2)	169.2(2)	171.8(2)
O(1)–P(1)–N(1)	103.8(6)	104.87(7)
O(1)–P(1)–C(1)	94.2(5)	93.39(7)
N(1)–P(1)–C(1)	104.8(5)	106.47(7)
O(2)–P(2)–N(2)		103.59(7)
O(2)–P(2)–C(2)		94.46(7)
N(2)–P(2)–C(2)		105.68(7)
C(9)–O(1)–P(1)	116.4(1)	116.9(2)
C(16)–O(2)–P(2)		115.8(2)

Scheme 3. Methanolysis of the *meta*-Carbaboranylbis(aminobromophosphine) **8a/b**



Spectroscopic Properties of 8a/b. Due to the larger distance between the two chiral phosphorus atoms (573.2 pm), only one signal is observed for the mixture of diastereomers in the $^{31}\text{P}\{^1\text{H}\}$ NMR spectrum at 127.2 ppm. The proton NMR spectrum is not different from that for the *ortho*-carbaborane analogue **4**. The $^{11}\text{B}\{^1\text{H}\}$ NMR spectrum shows four signals in a ratio of 2:3:3:2, which can be assigned according to the literature, where boron atoms closest to carbon atoms are observed at the lowest chemical shift and boron atoms furthest from carbon atoms at the highest.⁴⁴

Methanolysis of 8a/b. The diastereomeric mixture **8a/b** was then heated under reflux for 4 h according to the protocol for the *ortho*-carbaborane derivatives **2–5** with methanol as a solvent and triethylamine as a base (Scheme 3). A $^{31}\text{P}\{^1\text{H}\}$ NMR spectrum of the reaction mixture showed exclusive formation of methoxy-substituted compound **9a/b**. This result is in excellent agreement with the theory of missing P···P interactions. Separation of the diastereomers of **9**, which is a pale yellow oil, was unsuccessful.

An alternative approach for alkoxy-substituted *ortho*-carbaboranylbisphosphines is the reaction of the *ortho*-dilithiocarbaborane, with an alkoxy-substituted amidochlorophosphine having only one chlorine atom for substitution. This reaction pathway is more favored, because it has only one step instead of two, and therefore the total yield is higher than in the two-step synthesis discussed above.

The $^{31}\text{P}\{^1\text{H}\}$ NMR spectra of these compounds exhibit signals at 132.8 ppm (**6a**) and 126.1 ppm (**7b**), which is a markedly low-field shift in comparison to the halophosphine derivatives **2** and **3**. For the carbon atoms of the cluster, a triplet similar to compounds **1–5** is observed at 85.5 ppm (**6a**) and 87.7 ppm (**7b**). The sum of the direct and geminal C–P coupling constants amounts to 85.0 Hz (**6a**) and 80.9 Hz (**7b**).

Molecular Structures of 6a and 7b. Compound **7b** crystallizes in the orthorhombic space group $P2_12_12_1$ with four molecules in the unit cell and **6a** in the monoclinic space group $C2/c$ with four molecules in the unit cell. The structure of **6a** is shown in Figure 9, and **7b** is shown in Figure 10. Selected bond lengths and angles are listed in Table 7. The *rac* isomer **6a** has a crystallographic C_2 axis which bisects the C(1)–C(1a) and B(4)–B(4a) bonds. Due to the presence of an inversion center in this space group, both enantiomeric forms of **6a** (*R,R* and *S,S*) are present in the unit cell. The *meso* isomer **7b** has a mirror plane, which bisects the C(1)–C(2) bond.

The bond lengths are, overall, in the same range as those of the carbaboranylbis(halophosphines) presented above.

Conclusions

Novel amidohalophosphine derivatives of *ortho*-carbaborane were synthesized and fully characterized. The separation of the *rac* and *meso* diastereomers was successful in most cases, and therefore the configuration of the phosphorus atoms could be determined. Further functionalization of the phosphorus atom was studied for carbaboranylbis(amino-halophosphines) **2–5**. Due to the P–Cl bond, the compounds were expected to undergo rapid reactions with O or N nucleophiles, but instead it was found that alcoholysis is hindered. Quantum chemical calculations using DFT showed that inhibition of the alcoholysis is of kinetic and not of thermodynamic origin. The rate of the methanolysis of the disubstituted *ortho*-carbaborane derivatives is about 57–262 times lower than that of the corresponding mono-substituted derivatives. The reasons for these observations

are, on the one hand, the steric demand of the carbaborane core and, on the other hand, possible P···P interactions. SEN analysis gives values ranging from 0.026 to 0.059 between P1 and P2, on the same order of magnitude as a hydrogen bond in a water dimer. Visualization of the canonical molecular orbitals shows significant overlap of orbital fragments with the same sign and therefore supports the picture of a possible attraction between the phosphorus moieties. In accordance with this theory, a *meta*-carbaboranylbis(aminobromophosphine) was found to undergo smooth alcoholysis. An alternative approach for alkoxy-substituted *ortho*-carbaboranylbisphosphines is the reaction of the *ortho*-dilithiocarbaborane with an alkyl-substituted amidochlorophosphite. This reaction yields the desired product in one step and is therefore favored for the synthesis of *ortho*-carbaboranylbis(*N,N*-dialkylamidoalkylphosphonites).

Acknowledgment. We gratefully acknowledge support from the Deutscher Akademischer Austausch Dienst (DAAD doctoral grant for I.M.).

Supporting Information Available: Computational details for theoretical calculations. This material is available free of charge via the Internet at <http://pubs.acs.org>.

(43) Kilian, P.; Slawin, A. M. Z.; Woollins, J. D. *Chem.—Eur. J.* **2003**, *9*, 215–222.

(44) Hermanek, S. *Inorg. Chim. Acta* **1999**, *289*, 20–44.